

# The Effect of Solidity on a Tidal Turbine in Low Speed Flow

T Hernández-Madrigal<sup>#1</sup>, A Mason-Jones<sup>#2</sup>, T O'Doherty<sup>#3</sup>, DM O'Doherty<sup>\*4</sup>

<sup>#</sup>Cardiff Marine Energy Research Group, Cardiff University  
Queens Buildings, Newport Rd, Cardiff, Wales

<sup>1</sup>[HernandezMadrigalT@cardiff.ac.uk](mailto:HernandezMadrigalT@cardiff.ac.uk)

<sup>2</sup>[Mason-JonesA@cardiff.ac.uk](mailto:Mason-JonesA@cardiff.ac.uk)

<sup>3</sup>[ODoherty@cardiff.ac.uk](mailto:ODoherty@cardiff.ac.uk)

<sup>\*</sup>School of Engineering, University of South Wales  
Treforest, Pontypridd, Wales

<sup>4</sup>[Daphne.ODoherty@southwales.ac.uk](mailto:Daphne.ODoherty@southwales.ac.uk)

**Abstract**— Tidal Stream Turbines have been designed to operate in flows with high velocity,  $> 3m/s$ , where more power can be extracted. New designs have been proposed to make installations in sites with lower free stream velocity economically feasible. This paper considers how solidity affects the overall performance of a turbine when located under lower inflow conditions than the ones it was originally optimised for. The research proposes a design tool for pitch angle variation and an optimisation method when considering all the performance characteristics of a turbine.

**Keywords**— Turbine Solidity, Low Speed Flows, Tidal Energy, Performance Characteristics, Pitch Angle

## I. NOMENCLATURE

$c$	= Average chord length	$m$
$\rho$	= Density for water	$kg/m^3$
$P$	= Extracted mechanical power	$kW$
$V$	= Inlet velocity	$m/s$
$B$	= Number of blades	—
$\alpha$	= Pitch angle	$^\circ$
$C_p$	= Power coefficient	—
$\omega$	= Rotational velocity	$rad/s$
$D$	= Rotor diameter	$m$
$R$	= Rotor radius	$m$
$A$	= Rotor swept area	$m^2$
$\sigma$	= Solidity	—
$P_t$	= Theoretical mechanical power	$kW$
$C_t$	= Thrust coefficient	—
$\lambda$	= Tip speed ratio	—
$T$	= Torque	$kN \cdot m$
$C_\theta$	= Torque coefficient	—

## II. INTRODUCTION

The design of Tidal Stream Turbines (TSTs) is developed from the knowledge and experience gained within the wind energy, and is often based on the technology for three bladed turbines in open flows[1], among others. Part of a turbine's characteristics is defined by its solidity which has been used in wind energy to compare the performance characteristics of similar turbines with small variations in their blade geometry. Within tidal energy research, the solidity characteristic has

been used to select the right number of blades in a cross-flow turbine[2] and in a horizontal axis tidal turbine[3].

At the moment most of the research in TSTs is aimed at turbines that will be deployed in locations where the flow velocities are higher than  $2 m/s$ . However as the technology matures, this minimum velocity is decreasing as it becomes more economically feasible to develop projects in areas with flow velocities closer to  $1 m/s$ , such as Costa Rica[4].

Research presented in this paper therefore characterises the performance of a TST sited in locations where the free stream velocity is as low as  $1.2 m/s$ . Further work is focused on reducing the inflow velocity even more.

The UK and the rest of the world can benefit from the advance in devices that can work in such conditions, since the available sites would increase bringing also the possibility for more sites becoming economical viable and consequently more countries getting involved with tidal energy, from both the research and the industry perspective[5].

## III. SETUP

The turbine geometry from the Cardiff Marine Energy Research Group (CMERG), which has been characterised thoroughly in previous studies[6], has been used as a reference in this study. It is a three bladed horizontal axis tidal turbine with a Wortmann FX 63-137 aerofoil profile.

This work is made using computational fluid dynamics (CFD), by simulating the rotation of a turbine under the sea in conditions that resemble low speed flow,  $\sim 1.2 m/s$ . In this section the computational setup is detailed.

### A. Turbine

The purpose of this research is to determine what geometry configuration for the aforementioned turbine is the best to operate at  $1.2 m/s$  when its solidity is modified, considering its power output, loads, torque and rotational speed – its performance characteristics.

1) *Solidity*: Solidity,  $\sigma$  is defined as 'a term which loosely expresses the ratio of the surface area (one side) of the blades to the rotor swept area. The area is planform (chord and twist

distribution) and not a projected area on the rotor plane which would in general be less due to the blade twist distribution' [1]. The equation is given by:

$$\sigma = \frac{Bc}{\pi R} \quad \text{Eq. 1}$$

As a result, solidity can be changed by varying the number of blades, the average chord length (as used in Eq. 1) and/or the size of the rotor. For the purpose, a series of computational fluid dynamics (CFD) studies of a 10 m diameter turbine with an average chord length  $c = 1.1$  m were undertaken with the number of blades changed from 3 to 5 to vary the solidity from  $\sigma = 0.21$  for the 3 bladed turbine to  $\sigma = 0.35$  for the 5 bladed turbine. For simplicity the blade twist is not considered for the solidity calculations.

Morris et al [3] modelled the CMERG turbine with 2, 3 and 4 blades to obtain the highest power for the turbine operating with an inflow velocity of 3.1 m/s. The tip pitch angle was modified for each of the cases and the required tip pitch angle for maximum power was determined as 3°, 6° and 9°, respectively. Further work [6] done with Fluid-Structure Interaction (FSI) showed that for the 4 bladed turbine, the maximum power output happened with an increment of 0.2° over the 9° previously obtained.

However, a turbine needs to be optimised in terms of its power, torque and thrust loads. Therefore this original study has been extended to consider all these three performance characteristics and their suitability for a low speed turbine. Consequently the same turbine design has been used, but modified for 3, 4 or 5 blades. That is, the same original geometry for the blades and the hub were used and the 3, 4 and 5 bladed turbines were modelled with various pitch angles to determine what arrangement would be the optimum for the turbine, under a low speed velocity inflow of 1.2 m/s.

Using [6] as reference, the analysed tip pitch angles for the 4 bladed turbine are 9.2°, 10°, 11° and 18°. Following the trend, for the 5 bladed turbine, the selected tip pitch angles are 10°, 12°, 13° and 30°. The largest angles, i.e.  $\alpha = 18^\circ$  and  $\alpha = 30^\circ$ , for the 4 and 5 bladed turbines respectively, are the extreme cases modelled during the optimisation procedure.

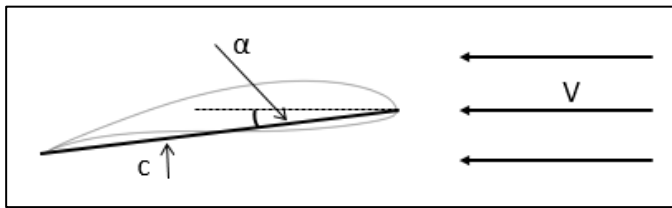


Fig. 1 Geometry variables in the blade profile

TABLE I  
TURBINES' SOLIDITY DETAILS

Turbine	$B$	$\sigma$	$\alpha$
A	3	0.21	6°
B	4	0.28	9.2°, 10°, 11°, 18°
C	5	0.35	10°, 12°, 13°, 30°

A summary of the geometry details for the turbines can be seen in TABLE I, and Fig. 1 illustrates the location of the geometrical variables within the blade profile.

2) *Performance characteristics*: The theoretically available power [1]  $P_t$  is dependent on the upstream velocity and is defined as

$$P_t = \frac{1}{2} \rho A V^3 \quad \text{Eq. 2}$$

Where  $\rho$  is the density of the water, which for the purpose of this research was 997 kg/m<sup>3</sup> in order to simulate the conditions used in the experiments that validate the results for the original CMERG turbine, fresh water at 20 °C.  $A$  is the swept area covered by the rotor which is 78.54 m<sup>2</sup> for a 10 m diameter tidal turbine, and  $V$  is the inflow velocity of the water which was set to 1.2 m/s.

In practice only some of the power can be extracted for the flow and the extracted power  $P$  is dependent on the torque and the rotational speed of the turbine. It is calculated using Eq. 3.

$$P = T \omega \quad \text{Eq. 3}$$

This allows the power coefficient  $C_p$ , which is the ratio of the extracted power to the theoretically available power, to be calculated, as given in:

$$C_p = \frac{P}{P_t} = \frac{2P}{\rho A V^3} \quad \text{Eq. 4}$$

In the same way, the thrust coefficient  $C_t$  is calculated, to normalise the axial or thrust load  $F$  acting on the turbine to the axial load over the swept area and is given by:

$$C_t = \frac{2F}{\rho A V^2} \quad \text{Eq. 5}$$

Finally, the torque coefficient is calculated, using Eq. 6, since this is helpful in determining the self-starting capability of the turbine [1], and the torque transmitted to the generator. It is of major importance for low speed flows, where low transmission losses are desired. A high enough torque is required to overcome the inherent losses in the system.

$$C_\theta = \frac{2T}{\rho A V^2 R} = \frac{C_p}{\lambda} \quad \text{Eq. 6}$$

The coefficient parameters were obtained for each of the CMERG turbine configurations tabulated in TABLE I and then compared for the different tip speed ratio  $\lambda$  (Eq. 7), and different pitch angles  $\alpha$ .

$$\lambda = \frac{\omega R}{V} \quad \text{Eq. 7}$$

3) *Analysis*: With these values in hand, the selection parameters for the optimum turbine configuration can be determined based upon the need of high power, high torque, and low thrust [1]. Consequently,  $C_p$ ,  $C_\theta$  and  $1/C_t$  need to be maximised for the optimal characteristics.

## B. CFD Model

This study was done with the CFD package of ANSYS Academic Research, Release 16.0. The mesh was created using ICEM CFD and to the simulations were ran with ANSYS CFX.

1) *Mesh*: To create the model, first the sea domain was meshed until the wake characteristics was considered independent of the number of elements added. Then, the turbine was meshed in a cylinder surrounding it that works as the boundary of the moving reference frame (MRF). Another independency study for the MRF was done modelling Turbine A with an inflow velocity of  $3.086 \text{ m/s}$  at the already known peak operation point:  $\lambda = 3.65$ , until the results were validated with the ones obtained in previous research[6]. Once those values were reached, that meshing procedure was followed for Turbines B and C.

The domain for the simulations has a 3-dimensional rectangular shape of  $10D \times 10D \times 40D$  with the turbine hub located  $5D$  above the seabed,  $10D$  downstream from the inlet. The turbine was therefore located in the middle of the water column, and the effects of any stanchion were not considered. This ensured that the turbine hydrodynamics were unaffected by the boundary conditions, including near wall effects (i.e. the no-slip consideration). The overall size of the domain and turbine ensured that the blockage effect is less than 1%.

Two meshing methods were used: Hexahedral elements in the far field and tetrahedral elements in the MRF. The hexahedral part of the mesh has  $\sim 3$  million elements with a higher density in the middle of the domain and an O-Grid that surrounds the MRF to smooth the transition from the tetrahedral finer elements close to the turbine to the hexahedral coarser elements located in the far field. The number of elements in the MRF varies from  $\sim 3.5$  to  $\sim 5$  million elements, depending on the number of the blades each rotor has.

The MRF is a cylinder surrounding the turbine with a diameter of  $1.4D$  and  $5.1 \text{ m}$  width. It is created to separate the immediate volume of the fluid that is known to be rotating around the turbine from the stationary far field that represents the rest of the sea. This is done to apply a change in the frame of reference and to connect the non-matching grids – hexahedral with tetrahedral elements [7].

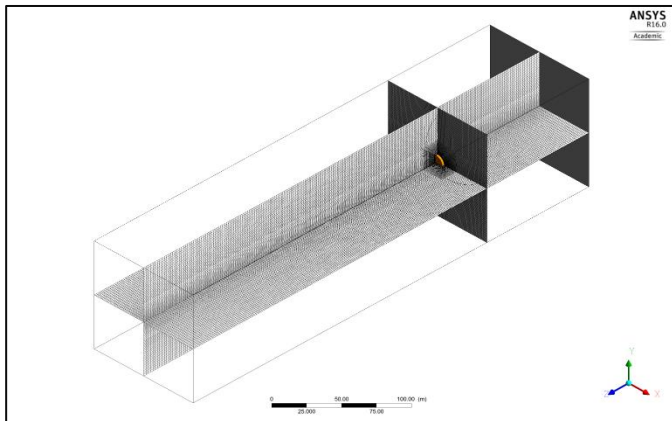


Fig. 2 Mesh cut planes of the whole domain

The mesh is shown in Fig. 2 and Fig. 3. The former demonstrates plane cuts of the whole model with the MRF highlighted to show its location, and the latter includes a zoom into the MRF to give an example of the mesh characteristics around the blades and hub of the turbine, which vary slightly depending on how many blades the turbine has. The inlet flow is the positive Z direction.

1) *Simulation Parameters*: The models were run in steady state mode with the intent of getting the performance characteristics of the turbines. It is considered that the turbine is operating at a constant rotational speed in a uniform flow field of constant velocity, following the actuator disc concept [1].

At the domain interface, the frozen rotor setup is used, which allows the interaction between the two different frames of reference, stationary with rotating. It changes the frame of reference from one component to the next whilst maintaining their relative position and making the required equation transformations [7].

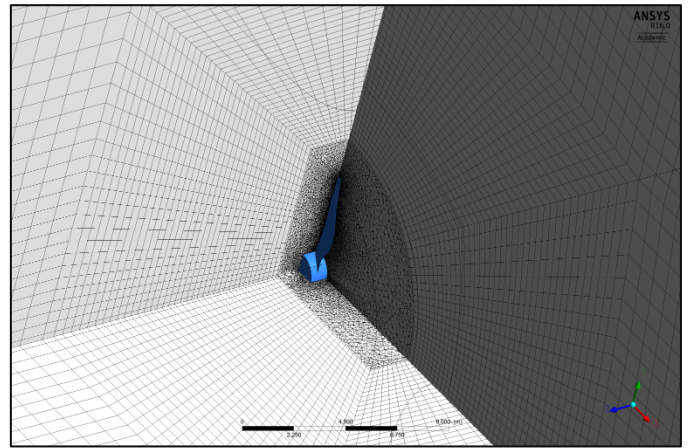


Fig. 3 Mesh of the MRF

The simulations were completed using the finite volume method, solving the Reynolds averaged Navier-Stokes (RANS) where attention is focused on the mean flow and the effects of turbulence on the mean flow properties[8], along with the *SST k - ω* turbulence model, which uses the *k - ω* model in the near-wall region and the standard *k - ε* model in the fully turbulent region far from the wall [8]. To the effects of this study, where there is no need to resolve the details of the turbulent fluctuations, the results provided by these equations are considered accurate.

2) *Boundary Conditions*: The models were set up with the following boundary conditions: -

- Inlet velocity of  $1.2 \text{ m/s}$ .
- Outlet relative static pressure of  $0 \text{ Pa}$ .
- Seabed set as No-slip wall.
- Surrounding sea set as Free-slip wall.
- Turbine blades and hub set as No-slip wall.

- Domain interface for the MRF set as General Connection Frozen Rotor with no pitch change.

#### IV. RESULTS

This section shows the gathered data and to find the peak operation point and the performance characteristics for the turbine configurations mentioned above.

##### A. Turbine A - Model Validation

First, Turbine A was simulated under the different inflow conditions to validate the model that was used for the other two turbines. The results were compared to previous studies where the turbine was characterised under different inflow conditions.

Considering the power coefficient as a reference it was determined that the model was accurate with a value of  $C_p = 0.45$ , a 5% difference to previous results [9] which can be attributed to higher mesh resolution in the present model, about 75% more elements in the MRF and 62% less elements in the sea domain, in total a 34% reduction in the number of elements.

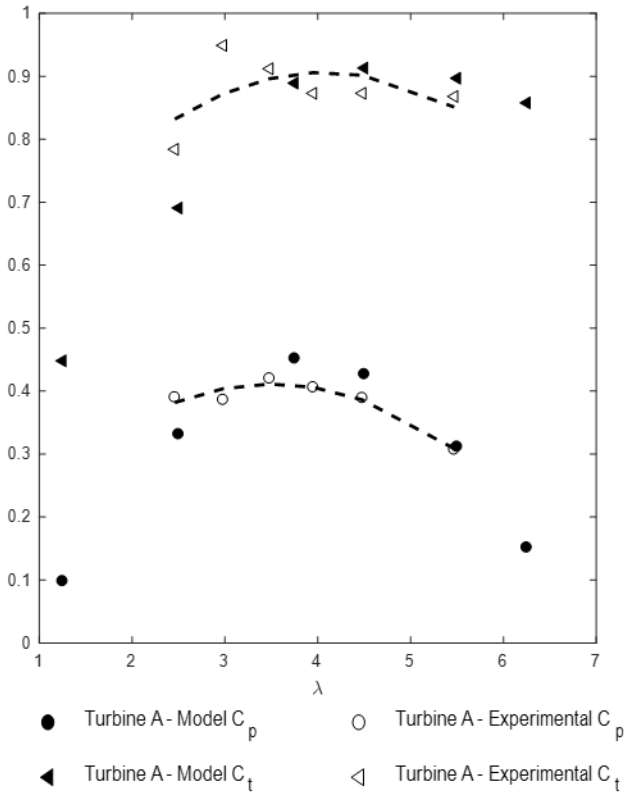


Fig. 4 Numerical model validation with previous experimental data

The numerical results obtained from the simulation of Turbine A have been validated against experimental data from Frost [10] and is shown in Fig. 4. The experimental values were obtained in the 220 m long INSEAN tow tank, with a towing speed of 1 m/s.

The  $C_p$  curve shows a good correlation with that of the experiment. The  $C_t$  data also has an overall good correlation

with those of the experimental data, with the exception of one data point. The full description of the experimental protocol can be found in [10] and [11]. This data provides the confidence in the results presented and discussed in this paper.

##### B. Turbine B

The 4 bladed turbine was modelled with five different tip pitch angles: 9.2°, 10°, 11°, and 18° at various values of  $\lambda$ . The first value of  $\alpha$  was taken as a starting point from the results Morris et al, obtained in their solidity study [3]. For a 4 bladed turbine rotating with an inflow velocity of 3.1 m/s they showed that peak power occurred at a tip pitch angle of 9.2°. Then  $\alpha$  was increased considering the trend in previous optimisation studies for wind turbines where it is seen that as the flow velocity decreases the peak  $C_p$  increases with the augmentation of the pitch angle [12].

The fluid upstream velocity provides the available theoretical power as defined by Eq. 2, tidal stream turbines are designed to extract as much mechanical power as possible. The CMERG turbine is designed to operate under 3.6 m/s flow conditions, which for a 10 m radius turbine results in 1832 kW of theoretically available power. In previous research [9], the device actually produced 786 kW under these design conditions ( $C_p = 0.43$ ).

With an upstream velocity of 1.2 m/s, which illustrates the conditions that are intended to be modelled following the Costa Rican sea characteristics, the theoretically available power reduces to 68 kW, therefore a turbine operating under such conditions must be optimised to extract the maximum power without unduly affecting the other performance coefficients of the turbine. The power coefficient varies depending on the pitch angle for the four bladed turbine (Fig. 5) such that as the tip pitch angle increases the maximum power coefficient decreases.

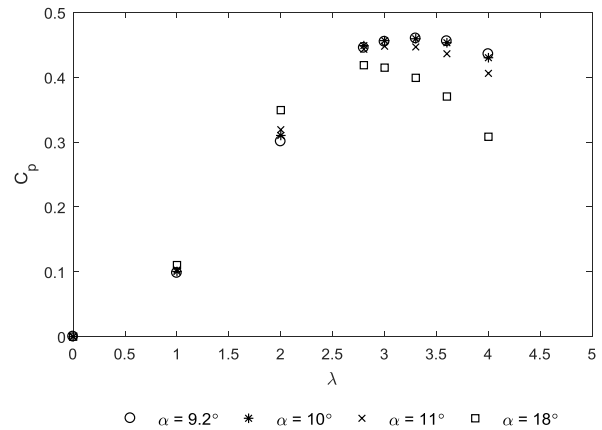


Fig. 5 Power coefficient curves for Turbine B

The maximum power is produced at the tip pitch angle of 9.2° as obtained from Morris et al [3] with a  $C_p$  value of 0.47. The peak  $C_p$  decreases slightly when the angle changes from 9.2° to 11°, a difference of 2.6%. As the tip pitch angle increases the peak  $C_p$  decreases, reaching a difference of 22%

when  $\alpha = 18^\circ$ . Also, the operation range shrinkages for the turbine. For Turbine B with  $\alpha = 9.2^\circ$  freewheeling occurs at  $\lambda = 5.6$ , whereas for the same blade with  $\alpha = 11^\circ$ , freewheeling occurs at  $\lambda = 5.1$ . Therefore the freewheeling tip speed ratio reduced as the tip pitch angle increases. In all the configurations that were modelled, the power curves overlap until the turbine reaches the peak operating point, which is slightly different depending on the tip pitch angle. As  $\alpha$  increases the peak shifts towards a lower tip speed ratio.

In Fig. 6 the variation of the thrust coefficient in relation to the tip speed ratio for Turbine B is shown. Up to  $\lambda = \sim 2.5$ , the curves for the 4 lowest tip pitch angles exhibit a similar behaviour and increase at the same rate. The lower the tip pitch angle, the more likely the peak thrust coefficient becomes constant between  $3 < \lambda < 4$ , after which the thrust coefficient decreases. The higher tip pitch angles reach a peak and immediately decrease. By relating Fig. 5 and Fig. 6 it is possible to see how a one degree change in the pitch angle causes a small variation of power output and a significant decrease of the thrust forces affecting the turbine. This will be discussed further in Section V.

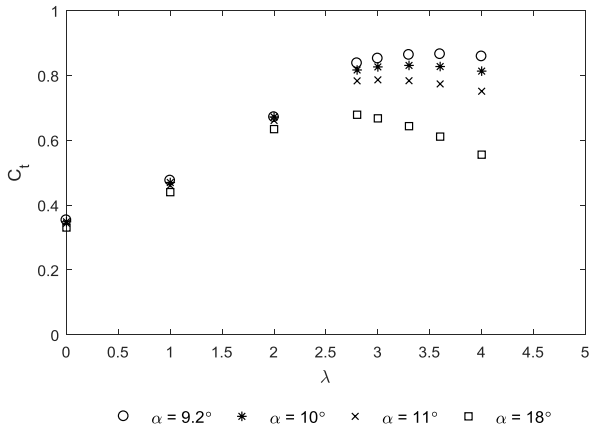


Fig. 6 Thrust coefficient curves for Turbine B

The torque coefficient curves for the 4 bladed turbine are presented in Fig. 7. The start-up torque is not affected by the pitch angle. A higher torque is achieved with a higher pitch angle, which can be beneficial for the generator requirements.

For  $\alpha = 9.2^\circ, 10^\circ$  and  $11^\circ$  the curves overlap with the curve shifting slowly towards the origin point. In normal operation conditions it is important to consider the steep decrease in torque as  $\lambda$  for peak power is reached. It is desirable to find the mechanical and economical balance between the torque and rotational speed of the turbine to maximise the generator power output. In order to reduce the costs the system should be as simple as possible, with minimal losses and maintenance risks, i.e. can the torque and rotational speed of the turbine match the generator specification without the need for a gearbox and provide an acceptable levelised cost of energy?

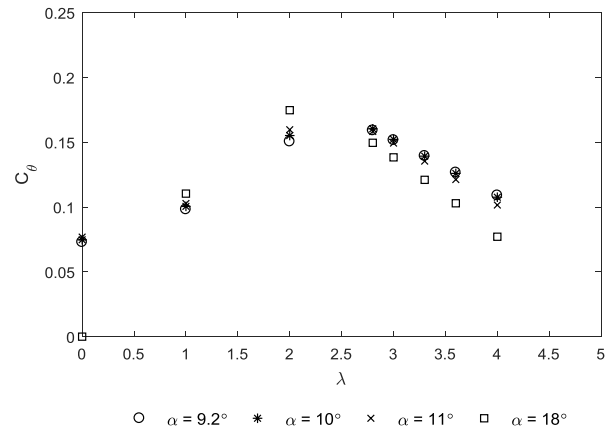


Fig. 7 Torque coefficient curves for Turbine B

### C. Turbine C

The 5 bladed turbine was also modelled at various values of  $\lambda$  with the blades oriented at different angles of  $\alpha$ :  $10^\circ, 12^\circ, 13^\circ$  and  $30^\circ$ . The tip pitch angles were determined extrapolating the angles used for Turbine B and correlating them to Turbine C.

The 5 bladed turbine was characterised in the same way Turbine B was. The power coefficient curves are shown in Fig. 8. Similar to the case of Turbine B, the curves overlap at the beginning of their operation range and start to separate as they get closer to their respective peak operation point.

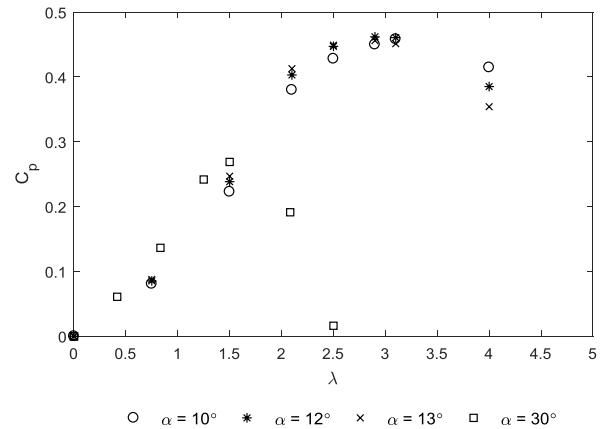


Fig. 8 Power coefficient curves for Turbine C

Turbine C produces the most power with the tip pitch angle of  $12^\circ$  where  $C_p = 0.46$ , but with a variation of a couple of degrees in  $\alpha$  there's only a decrease of 1% of the power coefficient. Also, as visible in Fig. 9, the thrust coefficient at peak power decreases 4% when  $\alpha$  changes from  $12^\circ$  to  $13^\circ$  and decreases 8% when  $\alpha$  changes from  $10^\circ$  to  $12^\circ$ .

With more blades, the turbine's operation range decreases as the tip speed ratio at freewheeling shifts to the left, and the tip speed ratio at peak power increases. For each added blade, the

peak power coefficient augments by 2%, a percentage that must be considered in regards to the real economic benefit.

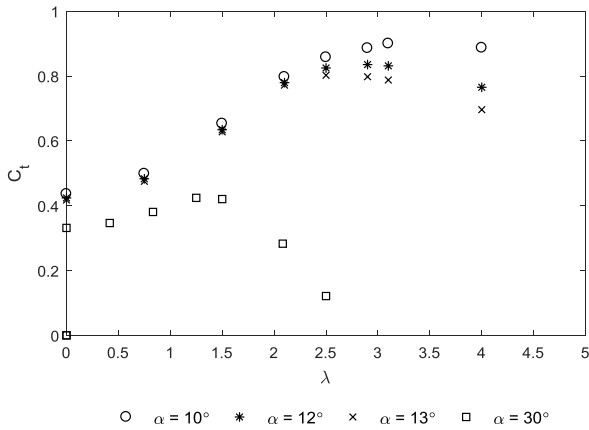


Fig. 9 Thrust coefficient curves for Turbine C

The torque coefficient for the 5 bladed turbine is shown in Fig. 10. The torque values are 25% higher than the ones for Turbine B, a factor to consider when the generator requirements get into consideration for a real tidal stream project.

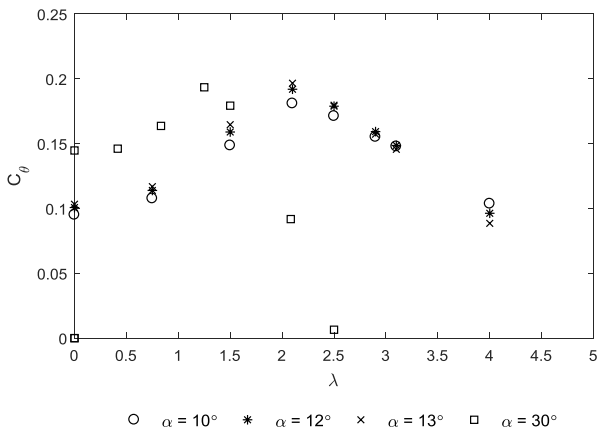


Fig. 10 Torque coefficient curves for Turbine C

To determine which turbine configuration is the best to operate at certain flow conditions, the number of blades, the tip pitch angle and the performance characteristics ( $C_p$ ,  $C_t$  and  $C_\theta$ ) must be analysed to identify the optimal turbine design for the location requirements.

It is important to recognise that along with the mechanical design parameters, economic feasibility studies should accompany the selection criteria for a specific site. Capital, maintenance and operation costs will be the decisive variables for a project to be viable.

The next section discusses how all the mechanical parameters can determine the best operation configuration for a specific design depending on the site characteristics.

## V. DISCUSSION

In Section IV the separate results for each turbine configuration were shown. It is clear from Fig. 5 to Fig. 10 that the larger the difference in the blade tip pitch angle the greater the change in the performance coefficients. This change is greater than the numerical error associated with grid dependency,  $\pm 2.5\%$ . With confidence gained from both validation and numerical accuracy, a direct comparison of the different scenarios has been made and a new turbine design tool proposed.

In Fig. 11 the power, thrust and torque coefficients are plotted together for the peak power conditions at different the various pitch angles modelled. For Turbine B and Turbine C the curves show how a small variation in the pitch angle can cause a small decrease of power whilst reducing the loads considerably. The torque coefficient is fairly constant as the pitch angle varies.

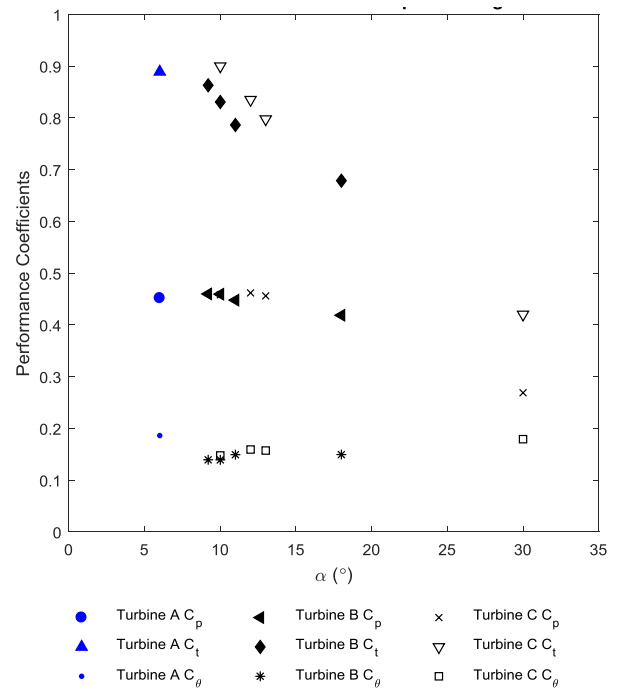


Fig. 11 Thrust and power coefficients at peak power

For Turbine B, the highest power extraction is obtained at  $\alpha = 9.2^\circ$ , if the tip pitch angle is increased to  $10^\circ$ , the thrust load can be reduced by 4% with a decrease of 1% in power. Even more, if the tip pitch angle is increased by a further  $1^\circ$ , the decrease in power would be 3% with a reduction in thrust load of 9%. As  $\alpha$  increases from the maximum power operation point the percentage power decrease also increases. On the other hand, the thrust keeps decreasing as the pitch angle increases.

If the solidity is increased further by the addition of another blade, as the case of Turbine C, a similar behaviour is seen. There is a 1% reduction of power and a decrease of 4% in the thrust load with  $1^\circ$  increase in tip pitch angle. The variation on

the power and thrust load with the tip pitch angle can be helpful when designing a turbine, since a small compromise in power can lead to a significant reduction in the thrust loads that the turbine must withstand, hence a drop in the manufacturing costs.

The curves shown in Fig. 11 can be used as a design and operation tool. Since they are made using geometrical non-dimensional parameters, they can be adapted for different flow conditions to know the power output and how much thrust load the turbine is withstanding.

When all the design coefficients are taken into consideration, an ‘optimum’ design can be outlined for the specific flow conditions. In order to choose which turbine configuration would be best for the  $1.2\text{ m/s}$  case that is analysed in the current study, Fig. 12 and Fig. 13 are used. They correlate the three design parameters detailed previously,  $C_p$ ,  $C_\theta$  and  $1/C_t$  – see Section III-A. From the design perspective, the optimum turbine would have the highest value for all the variables.

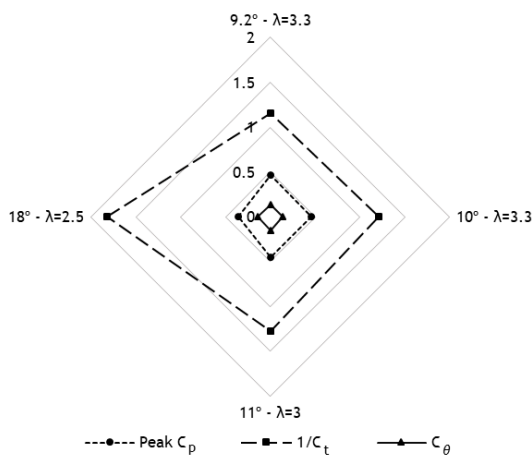


Fig. 12 Radar diagram to maximise design coefficients for Turbine B

For Turbine B, the highest power is obtained with a tip pitch angle of  $9.2^\circ$ , the same angle for an inflow of  $3.6\text{ m/s}$  [6], the highest torque coefficient at peak power is  $0.15$  and the highest  $1/C_t = 1.49$  occur at  $\alpha = 11^\circ$ . Since all the requirements are not under one specific tip pitch angle, with the graphs shown in these figures, it is possible to determine that a small compromise in power output can cause a considerable reduction in thrust. Therefore, to obtain the highest torque possible at peak operation, the  $11^\circ$  tip pitch angle is chosen as the Turbine B ‘optimum’ configuration. This selection would cause a decrease of  $3\%$  in the output power, but a reduction of  $9\%$  in the loads that the structure must withstand. It is also the angle with the highest torque at peak power.

In the case of Turbine C, as shown in Fig. 13, the highest power output is obtained when the 5 blades have a tip pitch angle of  $12^\circ$ , the highest  $C_\theta$  and  $1/C_t$  at peak power happens with  $\alpha = 30^\circ$ . However, a tip pitch angle of  $30^\circ$  gives a peak power  $42\%$  less than at  $12^\circ$ , therefore a compromise must be

done. Choosing the 5 bladed configuration with a tip pitch angle of  $13^\circ$  would cause a ‘loss’ in power but a reduction in the loads affecting the structure. It also entails a reduction in torque, which can be significant in low speed flows.

Comparing Turbine B and Turbine C at their selected pitch angles,  $11^\circ$  and  $13^\circ$  respectively, with Turbine A using  $\alpha = 6^\circ$  as it has been optimised previously [13], the power coefficient increases  $1.7\%$  for Turbine B and  $1.2\%$  for Turbine C, and the thrust coefficient decreases  $6.6\%$  for Turbine B and  $9.7\%$  for Turbine C. On the other hand, the torque coefficient decreases  $23.8\%$  for Turbine B and  $13.7\%$  for Turbine C.

This comparison shows that increasing the solidity by adding blades to a turbine operating in low speed flows, no major improvement in performance is made. The increase in power output and the decrease in loads are not as large as the loss in torque.

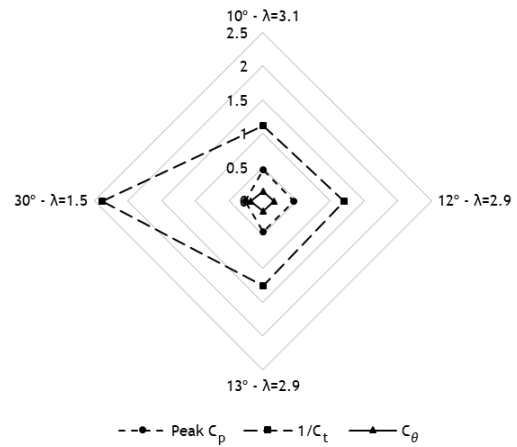


Fig. 13 Radar diagram to maximise design coefficients for Turbine C

Finally, in Fig. 14 the values of power and thrust load are seen for different inflow velocities and various pitch angles for Turbine B and C’s setup. The aforementioned curves can be used to define:

- The *optimum operation point* for which the turbine will be designed by maximising the power output whilst reducing the loads on the structure and keeping it economically feasible.
- If *pitch variation* during operation is worth considering in the design, and if so, to know how much power will be produced with the variation of the angle when done.
- The optimum *number of blades* depending on the flow conditions. The information shown in this paper along with the one data obtained by Mason-Jones [13] for the three bladed turbine pitch variation it is possible to optimise the device for different scenarios.
- Which *arrangement* is the most appropriate to operate in the selected location, by considering all the variables that are involved in the design.

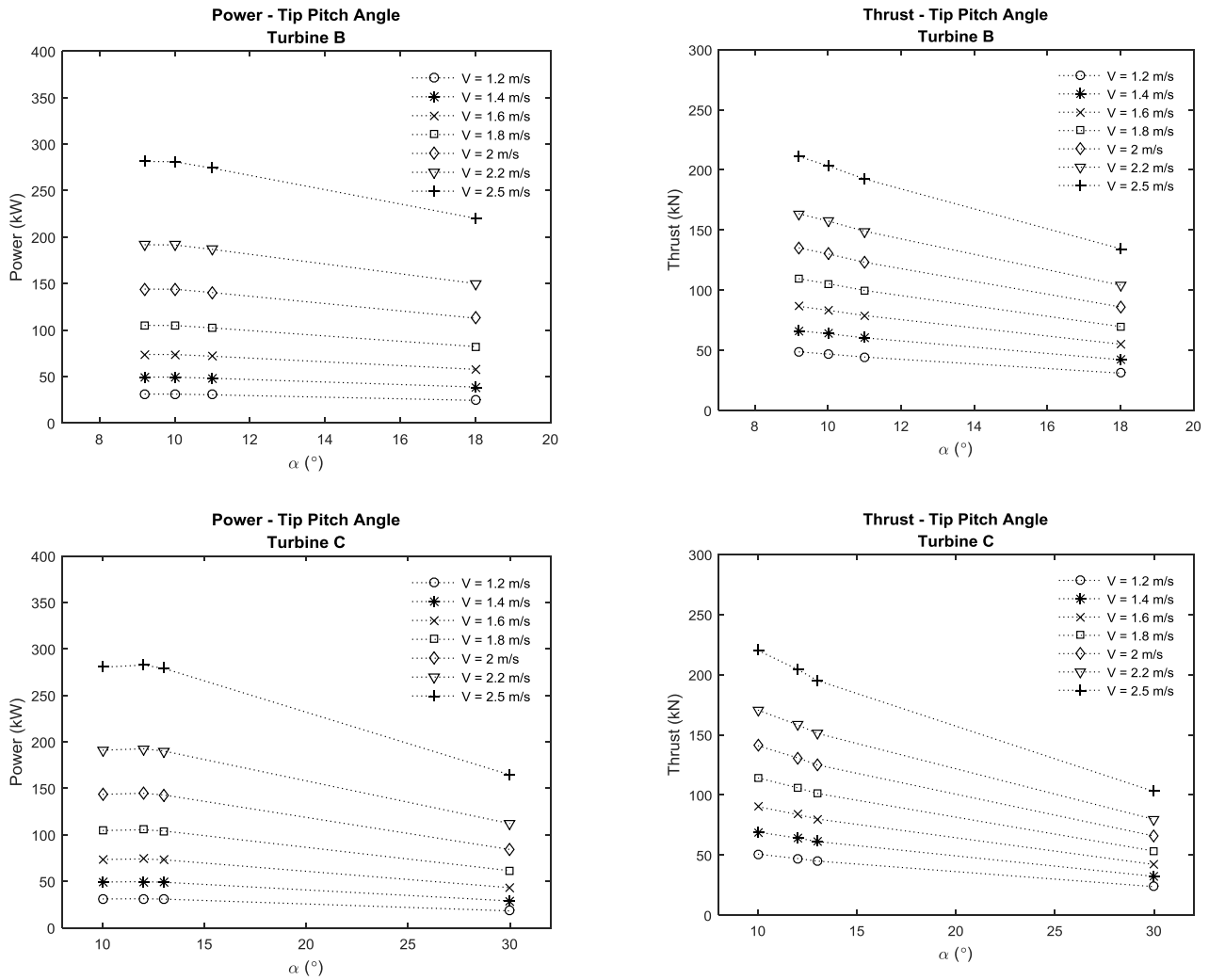


Fig. 14 Power and thrust curves at different inflow velocities for Turbine B and Turbine C

## VI. CONCLUSIONS

A study to determine how the solidity variation by changing the number of blades would affect a well characterised turbine operating at different inflow conditions was made. The turbine was modelled with one and two more blades than its original configuration, and the pitch angle was modified to obtain the optimum arrangement for each case, and for the inflow conditions of 1.2 m/s.

The power output range for different tip speed ratios decreased by adding blades and by increasing the pitch angle from the configuration with the highest peak power coefficient. The peak  $C_p$  was higher when more blades were added, and for each turbine when the pitch angle increased from the maximum peak power coefficient, the peak  $C_p$  was lower. The thrust load decreased when more blades were added and the  $C_t$  reduced as the pitch angle was higher from the peak power case. Finally, the lowest torque was obtained with the 4 bladed turbine, but

the 5 bladed turbine would still have lower torque than the original 3 bladed CMERG geometry.

A tool was proposed, where the variation of the pitch angle was plotted for the real power and thrust generated for a turbine in operation at several inflow velocities. These charts show how much the loads decrease by changing the pitch angle, whilst compromising a small power output. The charts can be used as a design or as an operation tool depending on whether the turbine is made with or without pitch variation. Along with these charts, a radar chart was made to show all the coefficients which affect the performance of a turbine and be able to choose the right combination by maximising all the variables involved. More parameters can be included in the radar charts, such as financial factors. The design parameters alone cannot establish which turbine is the best for low speed flows.

From the results of this work, the 3 bladed original turbine was considered the best configuration to operate in low speed flows. The other turbines provide a higher power output and less loads in the structure, but the reduction in the transmitted

torque did not justify the blades added because the increment in power was not high enough, < 2%.

#### ACKNOWLEDGMENT

Images used in Fig. 2 and Fig. 3 are courtesy of ANSYS, Inc. The authors gratefully acknowledge the financial support of Cardiff University for Ms Hernández-Madrigal.

#### REFERENCES

- [1] P. Jamieson, *Innovation in Wind Turbine Design*: Wiley, 2011.
- [2] C. Consul, R. Willden, E. Ferrer, and M. McCulloch, "Influence of solidity on the performance of a cross-flow turbine," in *Proceedings of the 8th European Wave and Tidal Energy Conference., Uppsala, Sweden, 2009*.
- [3] C. Morris, A. Mason-Jones, D. O'Doherty, and T. O'Doherty, "The Influence of Solidity on the Performance Characteristics of a Tidal Stream Turbine."
- [4] A. Brito e Melo, "INFORME FINAL - Costa Rica - Determinación del Potencial de Energía Marina para Generación Eléctrica," WavEC15 November 2013 2013.
- [5] H. Jeffrey, B. Jay, and M. Winskel, "Accelerating the development of marine energy: Exploring the prospects, benefits and challenges," *Technological Forecasting and Social Change*, vol. 80, pp. 1306-1316, 9// 2013.
- [6] C. Morris, "Influence of solidity on the performance, swirl characteristics, wake recovery and blade deflection of a horizontal axis tidal turbine," Cardiff University, 2014.
- [7] I. ANSYS, "ANSYS Academic Research," in *Help System*, Release 16.0 ed.
- [8] H. K. Versteeg and W. Malalasekera, *An introduction to computational fluid dynamics: the finite volume method*: Pearson Education, 2007.
- [9] C. Frost, P. Evans, C. Morris, A. Mason-Jones, D. O'Doherty, and T. O'Doherty, "Flow Misalignment and Tidal Stream Turbines," in *European Wave and Tidal Energy Conference 2015*, Nantes, France, pp. 09B2-5-1 to 09B2-5-6.
- [10] C. Frost, "Flow Direction Effects On Tidal Stream Turbines," Cardiff University, 2016.
- [11] S. Ordóñez Sanchez, K. Porter, C. Frost, M. Allmark, C. Johnstone, and T. O'Doherty, "Effects of extreme wave-current interactions on the performance of tidal stream turbines," 2016.
- [12] R. Lanzafame and M. Messina, "Fluid dynamics wind turbine design: Critical analysis, optimization and application of BEM theory," *Renewable Energy*, vol. 32, pp. 2291-2305, 11// 2007.
- [13] A. Mason-Jones, "Performance assessment of a horizontal axis tidal turbine in a high velocity shear environment," Cardiff University, 2010.